

allyl alcohol vs that of acrolein). Alternatively, one could argue that acrolein liberates vinyl groups and allyl alcohol liberates acetylene; the former would then lead to ethylidynes, ethylene, and ethane, but the latter to ethylidynes only. Candidates for elimination from saturated C₃ oxygenates include ethyl from propanal, and ethylidene (CH₃CH) or vinylidene (CH₂=C) from 1-propanol and propylene oxide.

A final note concerns the identity of the carbonyl-containing ligands liberated by C-C scission. If aldehydes decarbonylate via acyls, subsequent C-C scission in these will release CO directly. On the other hand, if the alcohols form strained oxametallacycle intermediates, it is difficult to imagine that complete dehydrogenation of the α carbon will precede ring-opening. Ring-opening prior to a C-H scission would release formaldehyde (H₂CO) or formyl (HCO) intermediates. Unfortunately these are quite difficult to detect under the conditions of these experiments; formyls have not been convincingly isolated on any single crystal transition metal surface, and formaldehyde dehydrogenates on Rh(111) at quite low temperatures (ca. 130 K^{26,32}), well below those of higher alcohol decomposition. If such species are indeed intermediates in higher alcohol decarbonylation, microscopic reversibility would suggest that higher alcohols might be synthesized by, for example, formyl addition to surface hydrocarbon ligands, rather than by the CO insertion step typically invoked by analogy with mechanism of homogeneous hydroformylation.

(32) Houtman, C.; Barteau, M. A. *Surf. Sci.* 1991, 248, 57.

Conclusions

The principal influences of the C=C group of allyl alcohol and acrolein are on the bonding configuration of these molecules on the Rh(111) surface and on the stability of the corresponding intermediates. Acrolein is adsorbed in an $\eta^4(\text{C,C,C,O})$ configuration and decarbonylates at lower temperatures than does its aliphatic analogue, propanal. Allyl alcohol dissociates to form allyl alkoxides which are bound in an $\eta^3(\text{C,C,O})$ configuration; these decarbonylate at higher temperatures than does *n*-propoxide. The decarbonylation selectivities of these reactants mirror those of their aliphatic counterparts, again demonstrating the divergence of the reaction pathways for alcohols and aldehydes. Acrolein, like the aliphatic aldehydes, gives rise to volatile hydrocarbon products one carbon shorter than the parent; neither allyl alcohol nor any primary alcohol produces volatile hydrocarbons on Rh(111). These results suggest that the hydrocarbon ligands and carbonyl moieties released by decarbonylation of aldehydes and alcohols on Rh(111) may differ, and that the corresponding synthesis of higher oxygenates may be similarly complex.

Acknowledgment. We gratefully acknowledge the support of this research by the Department of Energy, Office of Basic Energy Sciences, Division of Chemical Sciences (Grant FG02-84ER13290). We also thank Professor C. M. Friend for providing copies of refs 4-6 prior to publication.

Registry No. CH₂=CHCHO, 107-02-8; CH₂=CHCH₂OH, 107-18-6; Rh, 7440-16-6.

Dynamics of the Reaction CH₂OH⁺ → CHO⁺ + H₂. Translational Energy Release from ab Initio Trajectory Calculations

Einar Uggerud* and Trygve Helgaker

Contribution from the Department of Chemistry, University of Oslo, P.O. Box 1033 Blindern, N-0315 Oslo 3, Norway. Received September 25, 1991

Abstract: The classical equations of motion have been solved for the title reaction on the route leading from transition state to separated products using ab initio potential energy functions (HF and CASSCF). The calculations reproduce the experimentally observed translational energy release for both wave functions. Isotope effects on the translational energy release are also in good agreement with experiment. The calculations reveal that the translational energy release is a complicated function of the motion along the whole reaction trajectory. The situation at the transition state is not sufficient for predicting the final energy distribution.

I. Introduction

An important characteristic of unimolecular decompositions is the energy released as relative motion between the fragments.¹ When the reaction has a large barrier to the reverse reaction, the dominating source of the relative translational energy is the potential energy difference between the transition state and the separated products. The relative amount of this energy that ends up as translation is determined by the dynamics of the reaction. Therefore, the relative translational energy release² is a sensitive probe of the energy surface in the exit valley of the reaction. Of particular interest is the variation of the translational energy with isotopic substitution.

Large double focussing mass spectrometers are ideal for high-resolution measurements of translational energy release³ upon

fragmentation of ions. A large number of measurements have been carried out, but few investigators have been able to give their experimental observations the treatment needed for a precise analysis of the reaction studied.⁴ The most successful approach so far originates from Derrick and co-workers (vide infra).

Recently, we presented a method for integrating the classical equations of motion of the atoms in a molecular system on ab initio potential surfaces.⁵ Our method takes advantage of the fact that by using modern quantum chemical programs molecular gradients

(3) The amount of energy released in the form of relative motion of the two fragments will be termed translational energy release for reasons of simplicity. In many texts the term kinetic energy release is used for the same quantity.

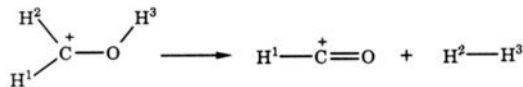
(4) For a review, see: Derrick, P. J.; Donchi, K. F. In *Comprehensive Chemical Kinetics*; Bamford, C. H., Tipper, C. F. H., Eds.; Elsevier: Amsterdam, 1983; Vol. 24, Chapter 2.

(5) Helgaker, T.; Uggerud, E.; Aa. Jensen, H. *J. Chem. Phys. Lett.* 1990, 173, 145-150.

(1) Polanyi, J. C. *Acc. Chem. Res.* 1972, 5, 161-168.
(2) Cooks, R. G.; Beynon, J. H.; Caprioli, R. M.; Lester, G. R. *Metastable Ions*; Elsevier: Amsterdam, 1973.

and Hessians are computed at a reasonable cost.⁶ It is therefore possible to perform realistic model calculations of the detailed motion of a reacting system. The trajectories obtained offer unique insight into the dynamics of a reaction. The quality of the model may be tested by comparing the calculated translational energy release with experimental data.

In this paper we discuss the reaction



which has been the subject of a series of experimental⁷ and theoretical⁸ investigations. From studies involving isotope labeling, the reaction mechanism has been shown to be a concerted 1,2-elimination of H₂, i.e., one of the hydrogens originates from the carbon atom and the other from the oxygen. The critical energies are 326 and 217 kJ mol⁻¹ for the forward and backward reactions, respectively. The high reverse barrier is reflected in the large translational energy accompanying the decomposition.

Experimentally, the translational energy release is determined from the shape of the metastable peak.^{2,9} The previously reported values for the fragmentation of protonated formaldehyde are in the range 1.42–1.44 eV.⁷ However, new methods for analyzing the effects of instrumental parameters on the shape of the metastable peak have revealed that these values are too low.¹⁰ Recent measurements reported by us¹¹ and March et al.¹² give a most probable translational energy release T_{mp} of 1.80 and 1.86 eV, respectively. A translational energy of 1.80 eV constitutes 80% of the reverse barrier.

To explain the large barrier in this and similar reactions, Hvistendahl and Williams applied molecular orbital symmetry conservation principles.^{7b} A symmetric 1,2-elimination of H₂ is forbidden by the Woodward–Hoffmann rules and should have a large barrier. Although this qualitative argument has some relevance, quantum chemical calculations at different levels of theory have revealed that H₂ does not depart from CH₂OH⁺ in a symmetrical fashion. In the transition state¹³ the OH bond is stretched more than the CH bond and the reaction center is tilted toward the carbon atom. Second-order Møller–Plesset (MP2) and complete active space self-consistent field (CASSCF) calculations using large basis sets reproduce the experimentally observed barrier quite satisfactorily.

These calculations agree well with the experimentally observed barrier but do not address the question of translational energy release, which is dynamical in its origin. We here present ab initio calculations of the classical trajectories of this reaction using our newly developed method. The relative translational energy is calculated upon separation of the fragments. Ab initio trajectories

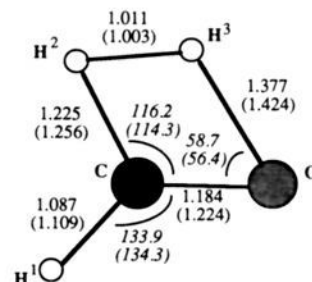


Figure 1. Transition-state geometry for loss of molecular hydrogen from protonated formaldehyde. Bond lengths are given in Å and bond angles in degrees. The indicated values refer to the Hartree–Fock transition state while the CASSCF transition-state geometry is given in parentheses.

are calculated for all possible deuterations and compared with existing experimental data.

The calculation of ab initio trajectories and translational energy releases makes it possible to investigate the relevance of the theory of Derrick and co-workers, in particular to what extent it is possible to predict the translational energy release solely from the dynamical situation at the transition state. In Derrick's theory, the relative translational energy release is taken to be that at the transition state, thus assuming that the motion away from the transition state does not influence the partitioning of the potential energy.

II. Computational Procedure

The method for calculating the molecular trajectories has been described elsewhere.⁵ We therefore restrict ourselves to a brief account. To determine a trajectory we solve Newton's equations of motion

$$\mathbf{m}\ddot{\mathbf{x}} = -\frac{dV(\mathbf{x})}{d\mathbf{x}} \quad (1)$$

Here $V(\mathbf{x})$ is the potential energy of the system and \mathbf{m} is a $3N$ -dimensional diagonal matrix containing the N nuclear masses:

$$\mathbf{m} = \text{diag}(m_1, m_1, m_1, m_2, m_2, m_2, \dots) \quad (2)$$

At some reference geometry \mathbf{x}^0 the molecular potential energy, gradient, and Hessian are evaluated ab initio. A second-order model surface is then constructed around the reference geometry

$$V_{\text{model}}(\mathbf{x}) = V_0 + \tilde{\mathbf{G}}\Delta\mathbf{x} + \frac{1}{2}\Delta\tilde{\mathbf{H}}\Delta\mathbf{x} \quad (3)$$

where

$$\Delta\mathbf{x} = \mathbf{x} - \mathbf{x}^0 \quad (4)$$

and V_0 is the molecular potential energy, \mathbf{G} the gradient, and \mathbf{H} the Hessian at \mathbf{x}^0 . Combining eqs 1 and 3 we obtain

$$\mathbf{m}\ddot{\mathbf{x}} = -\mathbf{G} - \mathbf{H}\Delta\mathbf{x} \quad (5)$$

This $3N$ -dimensional set of equations is diagonalized and the resulting $3N$ one-dimensional equations are solved analytically. In general, the model surface eq 3 is only valid in a small region around the reference geometry (the trust region) and the integration is carried out to the boundary of this region. The size of the trust region

$$h \leq \sqrt{\Delta\tilde{\mathbf{x}}\Delta\mathbf{x}} \quad (6)$$

is determined as described below.

The full trajectory is obtained in steps. In all calculations presented here, the trajectory is initiated at the transition state. The potential energy, gradient, and Hessian are calculated at the transition state and a second-order model surface is constructed. A small momentum is added along the reaction coordinate (the eigenvector belonging to the negative Hessian eigenvalue), and eq 5 is integrated to the boundary of the trust region on the product side of the transition state. The potential energy, gradient, and Hessian are then recalculated, a new model surface is constructed, and the trajectory is extended by integrating eq 5 to the boundary of the new trust region. This process is repeated until the fragments are well separated. The translational energy release is calculated from the relative velocity and reduced mass of the fragments. In practice, around one hundred iterations are needed for full separation of products.

Careful control of the trust radius h is necessary to ensure high numerical accuracy throughout the whole trajectory. In the course of the

(6) Helgaker, T.; Jørgensen, P. *Adv. Quantum Chem.* **1988**, *19*, 183–245.

(7) (a) Beynon, J. H.; Fontaine, A. E.; Lester, G. R. *Int. J. Mass Spectrom. Ion Phys.* **1968**, *1*, 1–24. (b) Williams, D. H.; Hvistendahl, G. *J. Am. Chem. Soc.* **1974**, *96*, 6753–6755. (c) Hvistendahl, G.; Uggerud, E. *Org. Mass Spectrom.* **1985**, *20*, 541–542.

(8) (a) Dewar, M. J. S.; Rzepa, H. S. *J. Am. Chem. Soc.* **1977**, *99*, 7432–7439. (b) Wijenberg, J. H. O. J.; van Lenthe, J. H.; Ruttink, P. J. A.; Holmes, J. L.; Burgers, P. C. *Int. J. Mass Spectrom. Ion. Proc.* **1987**, *77*, 141–154. (c) Hvistendahl, G.; Uggerud, E. *Org. Mass Spectrom.* **1991**, *26*, 67–73.

(9) A metastable peak is the signal observed in an energy spectrum of fragment ions formed from metastable ions. Metastable ions (in contrast to stable ions which survive the flight through the instrument) are ions which decompose during the flight through the mass spectrometer analyzer. For a large multiselector mass spectrometer, metastable ions have lifetimes of the order 1–10 μs .

(10) (a) Rumpf, B. A.; Derrick, P. J. *Int. J. Mass Spectrom. Ion Processes* **1988**, *82*, 239–257. (b) Koyanagi, G. K.; March, R. E.; Wang, J.; Snider, N. PS5—Kinetic Energy Release Deconvolution Package, Version 5.0, Trent University, 1990.

(11) Helgaker, T.; Hvistendahl, G.; Aa Jensen, H. J.; Schulze, C.; Uggerud, E. A Combined Theoretical and Experimental Approach to the Reaction Dynamics of H₂ Loss from Some Small Organic Ions. Poster presented at NATO ASI, Mont Ste. Odile, France, June 1990.

(12) March, R. E. Personal communication, September 1990.

(13) In this paper transition state is restricted to mean the stationary point at the molecular potential surface on the way between reactant and products where the Hessian (the second derivative matrix) has one negative eigenvalue.

Table I. Energy Data, Calculated and Experimental

molecule(s)	SCF			CASSCF			EXP $\Delta\Delta H^\circ$, ^g kJ mol ⁻¹
	energy, ^a hartree	$E(z.p.v.)$, ^b kJ mol ⁻¹	$E(rel)$, ^c kJ mol ⁻¹	energy, ^d hartree	$E(z.p.v.)$, ^e kJ mol ⁻¹	$E(rel)$, ^f kJ mol ⁻¹	
CH ₂ OH ⁺	-114.059 63	103.3	0	-114.201 36	96.2	0	0
transition state	-113.887 09	77.6	442 (428)	-114.052 32	73.5	391 (369)	326
CHO ⁺ + H ₂	-113.992 56	67.3	176 (140)	-114.169 26	61.4	84 (50)	109

^aHF/4-31G** data. ^bZero-point vibrational energy, from HF/4-31G** data, scaled by a factor 0.9. ^cRelative energies from the HF calculations, numbers in parentheses include zero point vibrational energy. ^dCASSCF/4-31G** data. ^eZero-point vibrational energy, from CASSCF/4-31G** data, scaled by a factor 0.9. ^fRelative energies from the CASSCF calculations, numbers in parentheses include zero point vibrational energy. ^gRelative heats of formation from the experimental data of ref 8c.

integration the anharmonicity of the potential surface is estimated by comparing the Hessians at adjacent points. In choosing the next step, the estimated anharmonic contribution to the energy of each mode is not allowed to exceed 1% of the harmonic contribution. The integration is also monitored by comparing the total kinetic energies calculated from the integrated momenta and from the conservation of energy. In no case did these differ by more than 0.1% at the end of the integration.

All trajectories were calculated by using a Hartree-Fock (HF) wave function constructed from a 4-31G** basis set.^{14,15} For the undeuterated species we also calculated the trajectory from a CASSCF wave function obtained by distributing 10 electrons in 10 orbitals.

III. Results and Discussions

We first determined the stationary points corresponding to the reactant, transition state, and products (see Figure 1 and Table I). The forward and reverse barriers are about 30% higher than the experimental values. This is to be expected since electron correlation is important for obtaining quantitative agreement for barriers. Static correlation improves the situation as can be seen from the CASSCF data, but some discrepancy remains due to basis set defects and neglect of dynamic correlation. Also, the experimental uncertainties are about 20 kJ mol⁻¹. The Hartree-Fock and CASSCF transition states are quite similar (see Figure 1). The transition-state geometry and reaction coordinate agree well with the experimental finding that the reaction is a concerted 1,2 elimination.

The kinetics of the reaction has recently been studied using the RRKM model at the Hartree-Fock level.^{8c} This investigation, which also takes into account quantum mechanical tunneling, shows that metastable CH₂OH⁺ ions do not possess any significant kinetic shift.¹⁶ The metastable ions therefore have a very narrow internal energy distribution, close to the threshold for fragmentation. In other words, the trajectories leading to fragmentation at the time scale of the experiment pass very close to the transition state. Moreover, at the transition state the atoms move slowly. Therefore, to analyze the products it is reasonable to start the calculations at the transition state with a small momentum added to each atom along the reaction coordinate. If sufficiently small (e.g., less than 10⁻⁴ atomic units), the initial momentum does not affect the outcome of the calculations.

The first trajectory was calculated at the HF level for the undeuterated species. The trajectory is illustrated in Figure 2 which shows a series of superimposed snapshots of the system on its way from transition state to products. Upon separation the relative velocity is 10.3 km/s, which gives a translational energy release of 83% of the calculated reverse barrier. The experimental value is 1.80 eV, corresponding to 80% of the observed reverse critical energy. Thus the relative translational energy is well reproduced.

To investigate the importance of correlation we calculated a trajectory at the CASSCF level. At this level 82% of the reverse critical energy is released as relative translation, indicating that the Hartree-Fock trajectory is qualitatively correct.

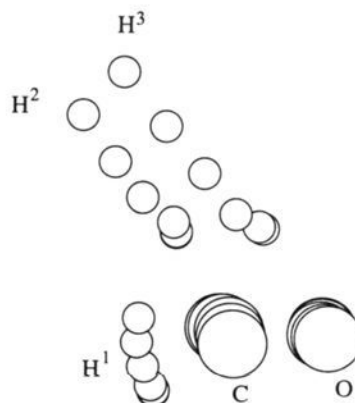


Figure 2. Geometries at six different times (0.0, 14.7, 20.1, 24.9, 30.0, and 35.0 fs, respectively) superimposed. The transition-state geometry is at the bottom. Hydrogens H² and H³ depart toward the upper left corner in the form of a dihydrogen molecule. Only 17% of the reverse critical energy is liberated as either internal vibration or relative rotation, the rest is given off as relative translational energy. Of the 17%, a large portion is given to the remaining hydrogen, H¹, in the form of a H-C-O linear bending motion.

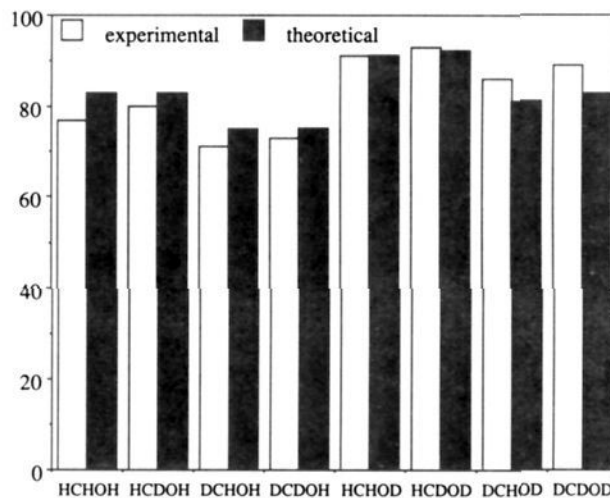


Figure 3. Relative proportion of the reverse critical energy liberated as relative translational energy of the two fragments formed from the eight isotopic species indicated. The ordering of the protium (deuterium) atoms from left to right is in accordance with the convention adopted in reaction I. The remaining hydrogen is the leftmost. The solid white columns represent the experimental data, while the hatched columns represent the results of the dynamical calculations. The experimental data are from ref 6c, and they have been scaled by a factor of 1.28 in accordance with recent measurements (see text) which show that the original method for obtaining translational energies gives systematically too low values.

(14) Hehre, W. J.; Ditchfield, R.; Pople, J. A. *J. Chem. Phys.* **1972**, *56*, 2257-2261.

(15) Frisch, M. J.; Pople, J. A.; Binkley, J. S. *J. Chem. Phys.* **1984**, *80*, 3265-3269.

(16) The excess (non-fixed) energy of the system as it passes over the transition-state region is sometimes termed the kinetic shift. The larger kinetic shift, the faster is the rate of decomposition of the molecule. See: Chupka, W. A. *J. Chem. Phys.* **1971**, *54*, 1936-1947.

Isotopic substitution influences the motion of the atoms of a molecular system, thereby affecting measurable properties of a reaction. For the reaction under investigation, isotopic shifts have been observed in the translational energy.^{7a,c} These shifts provide a sensitive test of the quality and reliability of the ab initio cal-

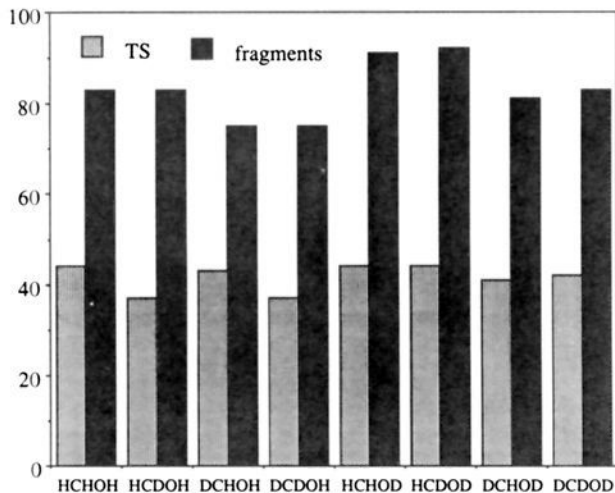


Figure 4. Relative translational energy release predicted from the situation after the first step away from the transition state (TS, light grey) and at the end of the trajectory (fragments, hatched). The ordering of the atoms is as explained in the legend of Figure 3.

culations. Therefore, in addition to the undeuterated calculation, we calculated one Hartree–Fock trajectory for each of the seven possible deuterated species. Figure 3 shows that the agreement between theory and experiment is very good for all eight isotopomers, the average deviation being only 3% (in absolute terms).

The largest calculated translational energies are observed when the hydrogen initially bonded to oxygen is substituted by deuterium. In contrast, the translational energy is significantly reduced upon deuteration of the non-departing hydrogen atom. Finally, deuteration of the hydrogen departing from carbon has little effect on the translational energy release. These isotopic shifts are in agreement with the experimental observations. We also note that the isotopic shifts appear to be additive, and more so for the calculated translational energies.

Although these calculations correctly predict relative translational energies as well as isotope effects, the details of the motion are hidden in the calculations. It would be useful if the application of a simpler physical model such as the one advocated by Derrick and co-workers¹⁷ would give similar predictions. Since Derrick's method is both conceptually simple and relatively easy to apply, we here compare it both with the experimental results and with our dynamical calculations.

Derrick's method was designed to account for the partitioning of the reverse critical energy into the product degrees of freedom. According to this method, the amount of energy entering the relative translation is determined by how well the reaction coordinate coincides with the product separation coordinate at the transition state. The product separation coordinate is the vector between the centers of mass of the fragments. Experience has proved the method to be quite successful in predicting translational energy releases. In particular, Rickard et al. have applied the theory to the elimination of H₂ from CH₂OH⁺.^{17a} To model the transition state they applied a MINDO/3 molecular potential (in contrast to the ab initio molecular potential applied in this work). Their results are in rather good agreement with the isotope effects

observed for the four isotopic species studied.

Provided the initial momentum is small, the prediction of Derrick's method is equivalent to the relative translational energy obtained in a trajectory calculation after the first step away from the transition state. Figure 4 compares the translational energy release predicted after the first step away from the transition state (equivalent to Derrick's original method when the atoms have zero kinetic energy initially) with the energy release as calculated upon fragmentation. The predictions at the transition state are clearly misleading, underestimating the relative translational energies by a factor of 2. The isotope effects are also poorly described. For example, the large isotope effect upon deuteration of the oxygen-bonded hydrogen atom is not reproduced from the transition state analysis.

Derrick's method works only if the overlap between the reaction coordinate and the product separation coordinate is conserved throughout the fragmentation. This is often not the case and success then depends on a cancellation of errors. This is illustrated by the experimentally observed negative secondary isotope effect of the nondeparting hydrogen. This may appear surprising. Although the two fragments carry the same momentum (oppositely directed) upon fragmentation, the hydrogen molecule carries 29/31 of the translational energy.¹⁸ We would therefore expect the motion of the light nondeparting hydrogen atom to have little effect on the translational energy release. However, the observed and calculated isotopic shifts clearly show that there is a strong coupling between the motion of the departing and nondeparting hydrogen atoms.

IV. Conclusions

We have studied the dynamics of the fragmentation of protonated formaldehyde at the ab initio level. Our calculations are in good agreement with experimental findings, and this process may therefore be considered well understood. In particular, we have been able to reproduce the experimentally determined relative translational energy release for the parent system and all possible deuterated species. We have found that the dynamical situation of the products cannot be derived from the situation at the transition state as assumed in the method by Derrick and co-workers. Integration of the dynamical equations along the complete trajectory is necessary in order to account for the translational energy release.

We have shown that the direct combination of ab initio electronic structure calculations with classical dynamics is both feasible and fruitful. This integrated approach bypasses the construction of the potential energy surface of the reactive system and therefore avoids arbitrary assumptions about the energy surface. By its very nature, this technique is restricted to classical dynamics since in quantum mechanics the calculation of the potential energy surface cannot be avoided. With increasing computer power it should become possible in the not too distant future to carry out full quasiclassical studies of molecular processes by carrying out a large number of ab initio classical trajectories. However, it already appears possible to study aspects of molecular dynamical processes such as translational energy releases at the ab initio level.

Acknowledgment. We thank VISTA (The Norwegian Academy for Science and Letters, and Statoil) and NAVF (The Norwegian Council of Science) for generous support.

Registry No. CH₂OH⁺, 17691-31-5; CHO⁺, 17030-74-9; H₂, 1333-74-0; D₂, 7782-39-0.

(17) (a) Rickard, G. J.; Cole, N. W.; Christie, J. R.; Derrick, P. J. *J. Am. Chem. Soc.* **1978**, *100*, 2904–2905. (b) Donchi, K. F.; Christie, J. R.; Derrick, P. J. *Adv. Mass Spectrom.* **1980**, *8*, 97–103. (c) Donchi, K. F.; Rumpf, B. A.; Willett, G. D.; Christie, J. R.; Derrick, P. J. *J. Am. Chem. Soc.* **1988**, *110*, 347–352.

(18) Cole, N. W.; Rickard, G. J.; Christie, J. R.; Derrick, P. J. *Org. Mass Spectrom.* **1979**, *14*, 337–340.